AD-A110 880 STATE UNIV OF NEW YORK AT BUFFALO FACULTY OF ENGINEER--ETC F/G 8/3
LONG OCEAN WAVE SCATTERING BY LINEAR SEGMENTED TOPOGRAPHIES.(U)
DEC 81 W L NEU, R P SHAW N00014-79-C-0067
UNCLASSIFIED 123 NL

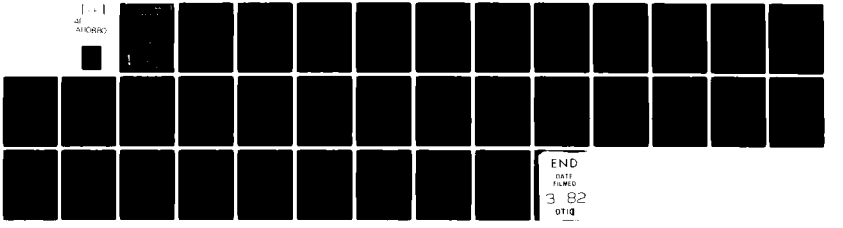

END
DATE FILMED
3 82
DTIC

LEVEL II

12

DEPARTMENT OF

ENGINEERING SCIENCE

AD A110880

DTIC
ELECTE
FEB 11 1982
S D
E

STATE UNIVERSITY OF NEW YORK AT

BUFFALO

82 02 11 059

LEVEL II (12)

Long Ocean Wave Scattering by Linear Segmented Topographies

W.L. Neu and R.P. Shaw

Dec. 1981

Rep. No. 123

This research was supported by the Office of Naval Research - Physical Oceanography under contract No. N0001479C0067.
Distribution is unlimited.

LONG OCEAN WAVE SCATTERING BY LINEAR SEGMENTED TOPOGRAPHIES

by

Wayne L. Neu and Richard Paul Shaw
Faculty of Engineering and Applied Science
State University of New York at Buffalo
Buffalo, New York 14260

ABSTRACT

Problems of transmission and reflection of long, time harmonic, free surface gravity waves obliquely incident from a constant depth ocean upon linearly varying bottom topographies are considered. A solution to the vertically integrated dynamic equations over linear depth variation is developed in terms of Kummer functions. Coriolis effects are included but primary interest is on Class I (high frequency) long waves. Three cases are treated; the continental slope and shelf, the submerged ridge and the submerged trench.

Introduction

This study considers the effects of three bottom topographies; the continental shelf and slope, submerged ridges and submerged trenches, on originally plane propagating long free surface gravity waves. In each case, linearized long wave theory for a homogeneous perfect fluid is used on one dimensional bottom topographies (parallel contours) which possess constant and linear cross sectional depth variations. The Coriolis effect due to the earth's rotation has been included in the theory. A distinction may be made on the basis of the wave frequency, ω, and the Coriolis frequency, f, between the two classes of long water waves. The Class I or inertiogravitational waves are characterized by $\omega >> f$. These waves can propagate in both directions along a N-S coast albeit with differing phase speeds for non-zero rotation and have periods which fall in the tsunami range and shorter, i.e., on the order of an hour or less. The Class II or quasi-geostrophic waves are characterized by $\omega << f$. These waves propagate in only one direction and cannot exist in the absence of rotation. They are an oceanographic scale phenomena with periods on the order of many hours or even days. This study is directed at the Class I waves where the Coriolis effect plays only a modifying role. Leblond and Mysak (1978) provide an important overview of the general area of ocean waves.

The solution utilized over linear depth variation was noted by Shaw (1974) and Guza and Davis (1974) in terms of Kummer functions, but no numerical results were given until Shaw (1977) due to an apparent lack of tables and/or subroutines for these functions. The application of this linear topography solution considered is that of long wave scattering by topographical features. Since these problems assume a progressive plane wave field incident from a semi-infinite ocean onto the feature to be studied,

the wave may not be trapped (within a linear theory). Wave trapping is studied in a related paper, Shaw and Neu (1981). Of interest here is the proportion of the incident wave energy reflected by or transmitted through the feature and the resulting wave amplitudes, especially at a coastline for the shelf-slope case.

The case of an infinite shelf, i.e., a slope connecting two constant depth regions with no coastline, was carried out by asymptotic methods by Voyt and Sebekin (1974) for an arbitrary monotonic depth in the slope region with the particular case of normal incidence and a linear slope carried out analytically. This problem has also been studied by Dean (1964) where the analytical solution for a linear slope and normal incidence was given without Coriolis effects and coastline. Shaw (1977) considered the case of long waves obliquely incident upon a linear slope and constant depth shelf which is terminated by a partially reflecting vertical wall. Recently, Abe and Ishii (1980) presented a similar solution to oblique incidence on a linear slope and, using a constant depth shelf, treat transmission and reflection problems in the cases of an infinite shelf and a shelf terminated by a rigid vertical wall. Refraction, diffraction and scattering are treated from a ray theory viewpoint by Murty (1977), who also provides a review of related work.

This study will develop the basic solution for long waves over a linearly varying bottom topography and apply this solution to problems of the transmission and reflection of waves obliquely incident upon submerged ridges and trenches as well as the continental slope and shelf where both slope and shelf have linear slopes and the shelf terminates with zero depth at the coastline.

Basic Formulation

The topographical features to be studied are assumed to have contours parallet to a y axis and a piecewise continuous cross section composed of segments whose depth varies linearly in an x direction. Although rotation on an f plane is included, the emphasis will be on first class surface gravity waves where Coriolis effects are a modifying rather than fundamental influence.

The vertically integrated equations governing long wave motion in water of variable depth, H, and Coriolis parameter f are, Lonquet-Higgins (1968),

$$\begin{aligned} \frac{\partial u}{\partial t} - fv &= -g\frac{\partial \zeta}{\partial x} \\ \frac{\partial v}{\partial t} + fu &= -g\frac{\partial \zeta}{\partial y} \\ \frac{\partial}{\partial x}[Hu] + \frac{\partial}{\partial y}[Hv] &= -\frac{\partial \zeta}{\partial t} \end{aligned} \tag{1}$$

where u and v are the horizontal particle velocities and ζ is the free surface elevation. Assuming a harmonic time dependence exp $-i\omega t$, equations (1) yield the following equation for ζ,

$$H\nabla^2\zeta + \frac{dH}{dx}\frac{\partial \zeta}{\partial x} + \frac{if}{\omega}\frac{dH}{dx}\frac{\partial \zeta}{\partial y} + \frac{\omega^2 - f^2}{g}\zeta = 0 \tag{2}$$

This equation may be non-dimensionalized with respect to some reference depth H_R and length L. This introduces the following non-dimensional quantities

$$\begin{aligned} \bar{h} &= H/H_R \quad , \quad (\bar{x},\bar{y}) = (x,y)/L \\ \bar{f} &= f/\omega \quad , \quad \bar{\omega} = \omega L/[gH_R]^{1/2} \\ \bar{\zeta} &= \zeta/H_R \end{aligned} \tag{3}$$

Equation (2) then becomes

$$\bar{h}\,\nabla^2\zeta + \frac{d\bar{h}}{d\bar{x}}\frac{\partial \bar{\zeta}}{\partial \bar{y}} + i\bar{f}\frac{d\bar{h}}{d\bar{x}}\frac{\partial \bar{\zeta}}{\partial \bar{y}} + \bar{\omega}^2[1 - \bar{f}^2]\bar{\zeta} = 0 \tag{4}$$

which will have different solutions for different topographies, $\bar{h}(\bar{x})$.

In each of the cases to be considered, it is assumed that the topographical feature is preceded by a region of constant depth H_1 over which the incident wave field travels. The depth H_1 shall be used as the reference depth. Thus in this region, $\bar{h}(\bar{x}) = 1$ and equation (4) becomes,

$$\nabla^2 \bar{\zeta} + \alpha^2 \bar{\zeta} = 0 \tag{5}$$

where we have set $\alpha = \bar{\omega} [1 - \bar{f}^2]^{1/2}$. A plane, unit, incident wave field whose normal makes an angle θ with the $\bar{x}$ axis is assumed of the form,

$$\bar{\zeta}_i = \exp [i \alpha \cos\theta \bar{x} - i \alpha \sin\theta \bar{y}].$$

Also present in this region will be a corresponding wave reflected from the topographical feature, traveling in the negative x direction and given by

$$\bar{\zeta}_r = R \exp[-i \alpha \cos\theta \bar{x} - i \alpha \sin\theta \bar{y}]$$

where R is the coefficient of reflection. Thus, the total wave field in this region is,

$$\bar{\zeta} = [\exp(i \alpha \cos\theta \bar{x}) + R \exp(-i \alpha \cos\theta \bar{x})] \exp(-i \alpha \sin\theta \bar{y}) \tag{6}$$

which satisfies equation (5). It is noted here that solutions in any region must have the same y dependence, therefore it will be dropped from future equations along with the explicit harmonic time dependence which has already been dropped.

In general, for a region of constant non-dimensional depth, $\bar{h}_c$, the governing equation becomes,

$$\bar{h}_c \nabla^2 \bar{\zeta} + \alpha^2 \bar{\zeta} = 0 \tag{7}$$

with solution,

$$\bar{\zeta} = C_1 \exp[-i\alpha(\frac{1}{\bar{h}_c} - \sin^2\theta)^{1/2} \bar{x}] \tag{8}$$

$$+ C_2 \exp[i\alpha(\frac{1}{\bar{h}_c} - \sin^2\theta)^{1/2} \bar{x}]$$

where C_1 and C_2 are arbitrary constants.

In regions of linearly varying non-dimensional depth defined by

$$\bar{h}(\bar{x}) = \delta + \gamma\bar{x} \tag{9}$$

where δ and γ are constants ($\gamma \neq 0$), equation (4) becomes,

$$(\delta + \gamma\bar{x})\, \nabla^2 \bar{\zeta} + \gamma \frac{\partial\bar{\zeta}}{\partial\bar{x}} + i\,\bar{f}\,\gamma \frac{\partial\bar{\zeta}}{\partial\bar{y}} + \alpha^2 \bar{\zeta} = 0 \tag{10}$$

Introducing a new variable, $z = \delta + \gamma\bar{x}$ and substituting for the $\bar{y}$ derivatives of $\bar{\zeta}$, this equation is,

$$z \frac{d^2\bar{\zeta}}{dz^2} + \frac{d\bar{\zeta}}{dz} + [\frac{\alpha^2 + \bar{f}\,\gamma\,\alpha\,\sin\theta - \alpha^2 \sin^2\theta\, z}{\gamma^2}] \bar{\zeta} = 0 \tag{11}$$

which is reducible to the confluent hypergeometric equation as seen in Chapter 6, section 2 of Erdelyi, et al. (1953). Two distinct cases must be considered. If $\theta = 0$, equation (11) corresponds to equation (8) of this reference and the solutions are,

$$C_o\ [2\alpha z^{1/2}/\gamma]$$

where C_o represents any two independent solutions to the zero order Bessel equation. If $\theta \neq 0$, we have the form of equation (6) of this reference with solutions,

$$\exp[-\xi/2] \cdot [F\ a,c,\xi]$$

where,

$$a = \frac{\gamma \sin\theta - \alpha - \bar{f}\,\gamma \sin\theta}{2\gamma \sin\theta} = \frac{1 - \bar{f}}{2} - \frac{\alpha}{2\gamma \sin\theta}$$

$$c = 1$$

$$\xi = \frac{2\alpha \sin\theta}{\gamma} z$$

F represents any two independent solutions to the confluent hypergeometric equation. Since c = 1, one of the solutions will be of logarithmic form. This form is appropriate for $\xi > 0$. For $\xi < 0$, the Kummer transformation leads to the form,

$$\exp[+ \xi/2] \cdot F[a', 1, -\xi]$$

where $a' = 1 - a = \frac{1 + \bar{f}}{2} + \frac{\alpha}{2\gamma \sin\theta}$.

The solution in regions of non-zero, constant slope bottom topography, for $\theta \neq 0$, is therefore (using the notation of Abramowitz and Stegun, 1964),

$$\begin{aligned} \bar{\zeta} &= \exp[-\xi/2]\,\{c_3 M(a,1,\xi) + c_4 U(a,1,\xi)\}; \quad \xi > 0 \\ &= \exp[+ \xi/2]\,\{c_3 M(a',1,-\xi) + c_4 U(a,1,-\xi)\}; \quad \xi < 0 \end{aligned} \tag{12}$$

where c_3 and c_4 are arbitrary constants. M and U represent the two independent Kummer functions. Programs to evaluate these functions have been written by and are available from the authors. These solutions may also be expressed in terms of Whittaker functions.

Continental Slope and Shelf

The first application considered is the reflection of a unit plane wave from a continental slope extending from $x = 0$ to $x = A$ and sloping shelf extending from $x = A$ to B. The shelf terminates with zero depth at the coastline, $x = B$. A cross section of the ocean, shown in figure 1, is divided into three regions,

Region I: $-\infty < x < 0$; $H(x) = H_1$

Region II: $0 < x < A$; $H(x) = H_1 - [H_1 - H_2]\, x/A$

Region III: $A < x < B$; $H(x) = H_2 \left[\frac{B - x}{B - A}\right]$

The reference length is chosen to be A and $\bar{h}_2 = H_2/H_1$, $b = B/A$ are defined.

The solution in region I, as given by equation (6) is,

$$\bar{\zeta}_I = \exp(i\,\alpha \cos\theta\, \bar{x}) + R \exp(-i\,\alpha \cos\theta\, \bar{x}); \qquad -\infty < \bar{x} < 0 \tag{13}$$

In region II, $\bar{h}(\bar{x}) = z = 1 - (1 - \bar{h}_2)\,\bar{x}$. Therefore, in equation (9), $\gamma = -(1 - \bar{h}_2)$ and the solution in this region ($\theta \neq 0$), from equation (12), is,

$$\bar{\zeta}_{II} = \exp[-\xi_2/2]\,\{A_2 M(a_2,1,\xi_2) + B_2 U(a_2,1,\xi_2)\}; \qquad \theta < 0$$
$$0 < \bar{x} < 1 \tag{14}$$
$$= \exp[\xi_2/2]\,\{A_2 M(a_2',1,-\xi_2) + B_2 U(a_2',1,-\xi_2)\}; \qquad \theta > 0$$

where A_2 and B_2 are constants and,

$$a_2 = \frac{1 - \bar{f}}{2} + \frac{\alpha}{2(1 - \bar{h}_2)\sin\theta}$$

$$a_2' = 1 - a_2 = \frac{1 + \bar{f}}{2} - \frac{\alpha}{2(1 - \bar{h}_2)\sin\theta}$$

$$\xi_2 = 2\alpha \sin\theta \left[\bar{x} - \frac{1}{1 - \bar{h}_2}\right] .$$

In region III, $\bar{h}(\bar{x}) = z = \bar{h}_2 \left[\frac{\bar{b} - \bar{x}}{\bar{b} - 1}\right]$, $\gamma = -\frac{\bar{h}_2}{\bar{b} - 1}$, and

$$\bar{\zeta}_{III} = \exp[-\xi_3/2] \{A_3 M(a_3,1,\xi_3) + B_3 U(a_3,1,\xi_3)\} \qquad \theta < 0$$

$$1 < \bar{x} < \bar{b} \qquad (15)$$

$$= \exp[\xi_3/2] \{A_3 M(a_3',1,-\xi_3) + B_3 U(a_3',1,-\xi_3)\} \qquad \theta > 0$$

where A_3 and B_3 are constants and,

$$a_3 = \frac{1 - \bar{f}}{2} + \frac{\alpha(\bar{b} - 1)}{2\bar{h}_2 \sin\theta}$$

$$a_3' = 1 - a_3 = \frac{1 + \bar{f}}{2} - \frac{\alpha(\bar{b} - 1)}{2\bar{h}_2 \sin\theta}$$

$$\xi_3 = 2_\alpha \sin\theta \, [\bar{x} - \bar{b}] \, .$$

However, as $\bar{x} \to \bar{b}$ ($\xi_3 \to 0$), $U \to -\infty$. Therefore, to insure a bounded solution at the coastline, B_3 must be set to zero. The solution in region III is then,

$$\bar{\zeta}_{III} = \exp[-\xi_3/2] \, A_3 M(a_3,1,\xi_3); \quad \theta < 0, \quad 1 < \bar{x} < \qquad (16)$$

$$= \exp[\xi_3/2] \, A_3 M(a_3', 1 - \xi_3); \quad \theta > 0$$

The evaluation of the coefficients R, A_2, B_2 and A_3 is accomplished by requiring continuity of the free surface elevation and mass flux at the interfaces $\bar{x} = 0$ and $\bar{x} = 1$. This introduces the following matching conditions,

$$\bar{\zeta}_I \, (\bar{x} = 0) = \bar{\zeta}_{II}(\bar{x} = 0)$$

$$\frac{\partial \bar{\zeta}_I}{\partial \bar{x}}(\bar{x} = 0) = \frac{\partial \bar{\zeta}_{II}}{\partial \bar{x}} (\bar{x} = 0) \qquad (17)$$

$$\bar{\zeta}_{II}(\bar{x} = 1) = \bar{\zeta}_{III}(\bar{x} = 1)$$

$$\frac{\partial \bar{\zeta}_{II}}{\partial \bar{x}} (\bar{x} = 1) = \frac{\partial \bar{\zeta}_{III}}{\partial \bar{x}} (\bar{x} = 1)$$

Equations (17) are four simultaneous algebraic equations in R, A_2, B_2, and A_3 which may be solved to complete the solution to the continental slope and shelf problem.

Submerged Ridge

The second problem considered is that of the transmission and reflection of a unit plane wave by a submerged ridge, which we divide into four regions:

Region I: $-\infty < x < -A$; $H(x) = H_1$

Region II: $-A < x < 0$; $H(x) = H_2 - [H_1 - H_2]\ x/A$

Region III: $0 < x < B$; $H(x) = H_2 + [H_3 - H_2]\ x/B$

Region IV: $B < x < +\infty$; $H(x) = H_3$

as shown in Figure 2. Again, A is used to scale horizontal distance and, $\bar{h}_2 = H_2/H_1$, $\bar{h}_3 = H_3/H_1$, and $\bar{b} = B/A$ are defined.

In region I, the solution is again given by equation (13) but applies to $-\infty < \bar{x} < -1$. In region II, $\bar{h}(\bar{x}) = \bar{h}_2 - (1 - \bar{h}_2)\ \bar{x}$, $\gamma = -(1 - \bar{h}_2)$ and the solution is

$$\bar{\zeta}_{II} = \exp[-\xi_2/2]\ \{A_2 M(a_2,1,\xi_2) + B_2 U(a_2,1,\xi_2)\}\ ;\quad \theta < 0\ ,\ -1 < x < 0 \qquad (18)$$

$$= \exp[\xi_2/2]\ \{A_2 M(a_2',1,-\xi_2) + B_2 U(a_2',1,-\xi_2)\}\ ;\ \theta > 0$$

where,

$$a_2 = \frac{1 - \bar{f}}{2} + \frac{\alpha}{2(1 - \bar{h}_2)\sin\theta}$$

$$a_2' = \frac{1 + \bar{f}}{2} - \frac{\alpha}{2(1 - \bar{h}_2)\sin\theta}$$

$$\xi_2 = 2\alpha \sin\theta \left[\bar{x} - \frac{\bar{h}_2}{1 - \bar{h}_2}\right]$$

In region III, $\bar{h}(\bar{x}) = \bar{h}_2 + (\bar{h}_3 - \bar{h}_2)\ \bar{x}/\bar{b}$, $\gamma = (\bar{h}_3 - \bar{h}_2)/\bar{b}$ and the solution is

$$\bar{\zeta}_{III} = \exp[\xi_3/2]\ \{A_3 M(a_3',1,-\xi_3) + B_3 U(a_3',1,-\xi_3)\}\ ;\quad \theta < 0\ ,\quad 0 < \bar{x} < \bar{b} \qquad (19)$$

$$= \exp[-\xi_3/2]\ \{A_3 M(a_3,1,\xi_3) + B_3 U(a_3,1,\xi_3)\}\ ;\quad \theta > 0$$

where,

$$a_3 = \frac{1 - \bar{f}}{2} - \frac{\alpha \bar{b}}{2(\bar{h}_3 - \bar{h}_2)\sin\theta}$$

$$a_3' = \frac{1 + \bar{f}}{2} + \frac{\alpha \bar{b}}{2(\bar{h}_3 - \bar{h}_2)\sin\theta}$$

$$\xi_3 = 2\alpha \sin\theta \left[\bar{x} + \frac{\bar{h}_2 \bar{b}}{\bar{h}_3 - \bar{h}_2}\right]$$

In region IV, $\bar{h}(\bar{x}) = \bar{h}_3$, a constant. If only the right-running transmitted wave is allowed in this region, the solution is given by

$$\bar{\zeta}_{IV} = A_4 \exp\left[i\,\alpha \left(\frac{1}{\bar{h}_3} - \sin^2\theta\right)^{1/2} \bar{x}\right] \; ; \quad \bar{b} < \bar{x} < \infty \tag{20}$$

If $H_3 > H_1$, then $\frac{1}{\bar{h}_3} < 1$ and if $\sin^2\theta > \frac{1}{\bar{h}_3}$, this solution becomes a decaying exponential. *In this case, no energy is transmitted in region IV.* The wave is totally reflected by the ridge. The critical incident angle, θ_{cr}, for such total reflection is defined by $\sin\theta_{cr} = \frac{1}{\sqrt{\bar{h}_3}}$, which agrees with Snell's law.

Thus, the solution in region IV is,

$$\bar{\zeta}_{IV} = A_4 \exp\left[i\alpha \left(\frac{1}{\bar{h}_3} - \sin^2\theta\right)^{1/2} \bar{x}\right] \quad \frac{1}{\bar{h}_3} > \sin^2\theta \; ; \quad \bar{\ell} < \bar{x} < \infty \tag{21}$$

$$= A_4 \exp\left[-\alpha \left(\sin^2\theta - \frac{1}{\bar{h}_3}\right)^{1/2} \bar{x}\right] \quad \frac{1}{\bar{h}_3} < \sin^2\theta$$

To determine the coefficients R, A_2, B_2, A_3, B_3 and A_4, continuity of free surface elevation and mass flux across the interfaces is once again required.

Submerged Trench

The submerged trench problem, Figure 3, is very similar to the submerged ridge problem. The four regions are defined by

Region I: $-\infty < x < -A$; $H(x) = H_1$

Region II: $-A < x < 0$; $H(x) = H_2 + [H_2 - H_1]\, x/A$

Region III: $0 < x < B$; $H(x) = H_2 - [H_2 - H_3]\, x/B$

Region IV: $B < x < +\infty$; $H(x) = H_3$

Again, A is used to scale horizontal distance and $\bar{h}_2 = H_2/H_1$, $\bar{h}_3 = H_3/H_1$ and $\bar{b} = B/A$ are defined. The solutions in each region are

$$\bar{\zeta}_I = \exp(i\,\alpha\cos\theta\,\bar{x}) + R\exp(-i\,\alpha\cos\theta\,\bar{x})\ ; \quad -\infty < \bar{x} < -1 \tag{22}$$

$$\bar{\zeta}_{II} = \exp[\xi_2/2]\,\{A_2 M(a_2',1,-\xi_2) + B_2 U(a_2',1,-\xi_2)\}\ ;\ \theta < 0\ ,\ -1 < \bar{x} < 0 \tag{23}$$

$$= \exp[-\xi_2/2]\,\{A_2 M(a_2,1,\xi_2) + B_2 U(a_2,1,\xi_2)\}\ ;\ \theta > 0$$

$$a_2 = \frac{1-\bar{f}}{2} - \frac{\alpha}{2(\bar{h}_2 - 1)\sin\theta}\ ,\ a_2' = 1 - a_2$$

$$\xi_2 = 2\,\alpha\sin\theta\,\left[\bar{x} + \frac{\bar{h}_2}{\bar{h}_2 - 1}\right]$$

$$\bar{\zeta}_{III} = \exp[-\xi_3/2]\,\{A_3 M(a_3,1,\xi_3) + B_3 U(a_3,1,\xi_3)\}\ ;\ \theta < 0\ ,\ 0 < \bar{x} < \bar{b} \tag{24}$$

$$= \exp[\xi_3/2]\,\{A_3 M(a_3',1,-\xi_3) + B_3 U(a_3',1,-\xi_3)\}\ ;\ \theta > 0$$

$$a_3 = \frac{1-\bar{f}}{2} + \frac{\alpha\bar{b}}{2(\bar{h}_2 - \bar{h}_3)\sin\theta}\ ,\ a_3' = 1 - a_3$$

$$\xi_3 = 2\alpha\sin\theta\,\left[\bar{x} - \frac{\bar{h}_2\bar{b}}{\bar{h}_2 - \bar{h}_3}\right]$$

$$\bar{\tau}_{IV} = A_4 \exp[i\,\alpha\,(\frac{1}{\bar{h}_3} - \sin^2\theta)^{1/2}\,\bar{x}]\;;\quad \frac{1}{\bar{h}_3} > \sin^2\theta\;,\quad \bar{b} < \bar{x} < \infty \qquad (25)$$

$$= A_4 \exp[-\alpha\,(\sin^2\theta - \frac{1}{\bar{h}_3})^{1/2}\,\bar{x}]\;;\quad \frac{1}{\bar{h}_3} < \sin^2\theta$$

The same matching equations are once again used to find the coefficients R, A_2,B_2,A_3,B_3 and A_4.

Results

Continental Slope and Shelf

The effect of rotation is considered first. Figure 4 is a plot of the amplification of the incident wave at the coast versus the incident angle, θ, for periods (T) of 900, 1200, 2400, and 4800 seconds, each over the same topography at latitudes of 0 and 60 degrees. At zero latitude, where no Coriolis effect is present, the curves are symmetric about $\theta = 0$. As rotation is introduced, the curves shift slightly and become asymmetric. It is interesting to note that the 2400 second period curve shifts in a direction opposite that of the other three. It is seen that the Coriolis effect is larger for the longer period waves than for the shorter; however even at the rather large latitude of 50 degrees, the effect is small for the class I type wave periods of interest here. All further results therefore will be taken without Coriolis effects, i.e., f equal to zero.

It is now convenient to define

$$\lambda = T\sqrt{gH_2} \tag{26}$$

where T is the wave period. This λ is the wavelength at the edge of the shelf ($x = A$). It was found that the amplification at the coast, as a function of incident angle, is dependent upon the ratio of the shelf length to λ, $\frac{B - A}{\lambda}$, and the ratio $\bar{h}_2$. There is also a slight dependence upon the length A. The amplification at the coast at zero incident angle is plotted versus $\frac{B - A}{\lambda}$ for values of $1/\bar{h}_2$ of 15, 25, and 35 in figure 5. This curve clearly shows the cyclic behavior and resonance peaks of the amplifications. As $\frac{B - A}{\lambda}$ is increased, the cycle repeats at intervals of just under 0.25 with each cycle slightly higher and with a larger peak than the last. The amplitude of the peaks also increases with $1/\bar{h}_2$.

Figures 6 and 7 illustrate the angular dependence of the amplification. They are plots of the amplification at the coast versus the incident angle through one cycle of Figure 5, from $\frac{B - A}{\lambda} = 0.8$ to 1.05 in steps of 0.025 and at $1/\bar{h}_2 = 25$. Only $\theta \leq 0$ is shown due to the symmetry. The general shape of the curves repeat with each cycle. The curves from $\frac{B - A}{\lambda} = 0.8$ to 0.925, shown in Figure 6, are monotonic with the maximum at $\theta = 0$. These curves correspond to points to the left of a resonance peak in Figure 5, on an upward slope. In Figure 7, the curves correspond to points to the right of a resonance peak on a downward slope. They are no longer monotonic in θ, but have maximums away from zero near $\theta = -15$, -45, -60, and -75 for $\frac{B - A}{\lambda} = 0.95$, 0.975, 1.0, and 1.025 respectively. The curve $\frac{B - A}{\lambda} = 1.05$ corresponds to the $\frac{B - A}{\lambda} = 0.8$ curve and completes the cycle.

The differences in the slopes of the curves to the left and to the right of a resonance peak may be heuristically explained as follows. As the magnitude of θ increases, the wavelength perpendicular to the coastline, corresponding to λ in Figure 5, also increases. Thus, the ratio of the shelf length to the perpendicular wavelength is always less than or equal to $\frac{B - A}{\lambda}$. Referring to Figure 5, at a point to the left of a resonance peak, e.g., $\frac{B - A}{\lambda} = 0.9$, the ratio of shelf length to perpendicular wavelength, when $|\theta| > 0$, is to the left of 0.9 in a region of less amplification. At a point to the right of the peak, e.g., $\frac{B - A}{\lambda} = 0.975$, the shelf length to perpendicular wavelength is in a region of greater amplification. These waves encounter a resonance peak at an angle away from zero. In the case of $\frac{B - A}{\lambda} = 0.975$, it is near $\theta = -45$. These maximum amplifications away from $\theta = 0$ are more predominant in waves of shorter periods where the resonance peaks of Figure 5 are larger. Of course, this so called perpendicular wavelength is difficult to define due to the fact that the wave is turning in toward the coast as it moves up the slope and shelf, however a qualitative understanding of the phenomenon may be reached through the above argument.

Submerged Ridge

Figures 8 and 9 are plots of the magnitude of the reflection coefficient, R, versus the incident angle for several periods. The transmission coefficient is inferred by R since energy must be conserved. The ridge is symmetric with dimensions roughly coinciding with those of the Mid-Atlantic Ridge; $H_1 = H_3 = 5$ km, $H_2 = 2$ km, A = B = 100 km. For waves whose lengths are on the order of the total width of the ridge, the behavior is similar to the T = 900 sec. curve. As the period (and wavelength) is increased, a point of zero reflection develops and the ridge acts similar to a band-pass filter. This point of zero reflection moves inward along the incident angle axis with increasing period until reaching a point, $|\theta| \approx 53^{\circ}$ in this case, where it becomes relatively stationary. The shape of the curves in the region where $|\theta|$ is less than the point of zero reflection changes steadily from a shape of which the T = 1200 sec. curve is typical, where the reflection rises to a local maximum then drops off as θ approaches 0, to a monotonically increasing curve as in T = 2100 sec. As the period is increased beyond this point, the shape of the curves remains fairly constant with the reflection at $\theta = 0$ rising to a maximum then slowly falling off as seen in Figure 9.

In Figure 10, an asymmetric ridge is considered, illustrating the possibility of total reflection. Here, $H_1 = 5$ km, $H_2 = 2$ km, $H_3 = 6.5$ km, A = 100 km, and B = 120 km. The critical angle for an incident wave traveling in region I to be totally reflected is 61.29°. For angles of magnitude less than the critical angle, the curves retain a shape similar to the corresponding curves in the symmetric case. Notice that the rise to total reflection is very steep, most of which occurs in an interval of about 10 degrees.

Submerged Trench

Again, the magnitude of the reflection coefficient is plotted versus the incident angle for several values of T in Figures 11 and 12. The trench is symmetric with $H_1 = H_3 = 5$ km, $H_2 = 9$ km, A = B = 100 km. As in the ridge problem, there is a point of zero reflection, however it is present at the period of 900 sec. occurring at about $|\theta| = 35^{\circ}$. As the period is increased, the point of zero reflection moves out to about $|\theta| = 39^{\circ}$ where it remains relatively stationary. Notice also that the T = 900 sec. curve has very little reflection for incident angles of magnitude less than the point of zero reflection. The other major difference from the ridge problem is that at sharp angles, the smaller period waves are almost totally reflected. This is due to the fact that they are turned back out away from the trench by the slope of region II. As the ratio of H_2 to H_1 is increased, this reflection will increase.

In Figure 13, an asymmetric trench is considered. Although the possibility of total reflection exists in the trench problem when $H_3 > H_1$ as in the ridge problem, a model of the Japan Trench was chosen here with $H_3 < H_1$. The dimensions are: $H_1 = 6$ km, $H_2 = 9.5$ km, $H_3 = 3$ km, A = 60 km, B = 90 km. Note that in this case, only the T = 1800 sec. curve has a point of zero reflection. The other curves turn back up before reaching zero. In general, the reflections are larger than in Figures 11 and 12 for the angles of lesser magnitude, due to the shallower depth H_3, and smaller for angles of greater magnitude due to the smaller ratio of H_2 to H_1.

Conclusion

This presentation deals with an analytical study of a set of physical problems. No comparison is made at this time to observed oceanographic behavior. Long wave measurements across ridges and trenches are sparse; however it is clear that long waves actually do traverse ridges and trenches as they cross the ocean, e.g., tsunamis, and some reflection and transmission of energy must occur.

The amplification of wave heights at a coastline is more readily observed, but deep water wave amplitudes, measurements from which these coastal values are obtained, are again sparse -- even for the important case of tsunamis. The present analytical solution presents a "transfer function" representing the effect of the continental shelf-slope topography on an incident wave, i.e., the effect of shelf resonances by selectively amplifying certain frequencies. This transfer function transforms the deep water spectrum to a coastline spectrum for a plane incident wave but is dependent on the incident angle as well as the topography. Assuming the topography to be known, knowledge of the coastline spectrum and the original incident angle would allow reconstruction of the deep water spectrum. Abe (1981) has attempted to identify an incident angle but for tsunami sources on the same shelf as the observation points; the reconstruction here would require a distant source mechanism. Such problems are presently being studied.

Acknowledgement

The support of the Office of Naval Research-Physical Oceanography under contract No. N0001479C0067 for this work is gratefully acknowledged.

References

Abe, K. and H. Ishii, 1980. Propagation of tsunami on a linear slope between two flat regions. Part II reflection and transmission. J. Phys. Earth, 28: 543-552.

Abe, K., 1981. Incident angle identification from the spectrum for a tsunami invasion to the shelf. Bull. Nippon Dental Univ., Gen. Ed., 10(3): 87-93.

Abramowitz, M. and I.A. Stegun, 1964. Handbook of Mathematical Functions, NBS App. Math. Series 55, U.S. Dept. of Commerce.

Dean, R. 1964. Long wave modification by linear transitions. ASCE, Vol. 90, No. WW1.

Erdelyi, A., et al. 1953. Higher Transcendental Functions, Vol. 1, Bateman Manuscript Project, McGraw Hill Book Co., New York.

Guza, R.T. and R.E. Davis, 1974. Excitation of edge waves by waves incident on a beach. J. Geophys. Res., 79: 1285-1291.

LeBlond, P.H. and L.A. Mysak, 1978. Waves in the Ocean, Elsevier Oceanography Series, Elsevier Scientific Publishing Co., New York.

Longuet-Higgins, M.S. 1968. Double Kelvin Waves with Continuous Depth Profiles. J. Fluid Mech., Vol. 34(1), pp. 49-80.

Murty, T.S. 1977. Seismic Sea Waves: Tsunamis, Dept. of Fisheries and Marine Service, Ottawa, Canada.

Shaw, R.P. 1974. Long Waves on Linear Topographies. JTRE Internal Report No. 119, Haw. Inst. of Geophysics, Honolulu, Hi.

Shaw, R.P. 1977. Long waves obliquely incident on a continental slope and shelf with a partially reflecting coastline. IUGG Tsunami Symposium, Ensenada, Mexico (also see 1979 Marine Geodesy 2(1): 1-14).

Shaw, R.P. and W. Neu 1981. Long Wave Trapping by Linear Ridges, Jour. Phy Ocean. (in press).

Voyt, S.S. and B.I. Sebekin 1974. On the influence of bottom topography on the amplification of long waves. Proc. IUGG Tsunami Symposium, Wellington, New Zealand, Jan. 1974.

TABLE OF FIGURES

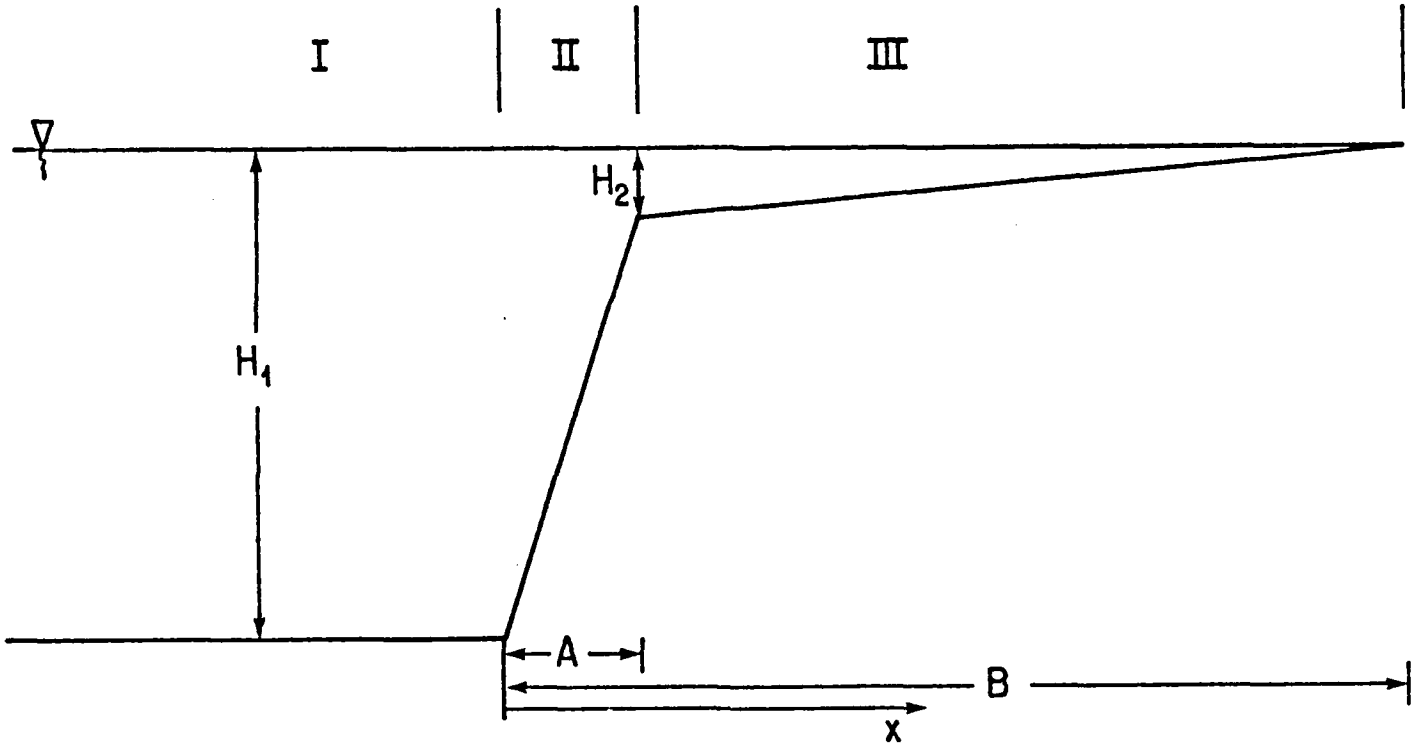

Figure 1

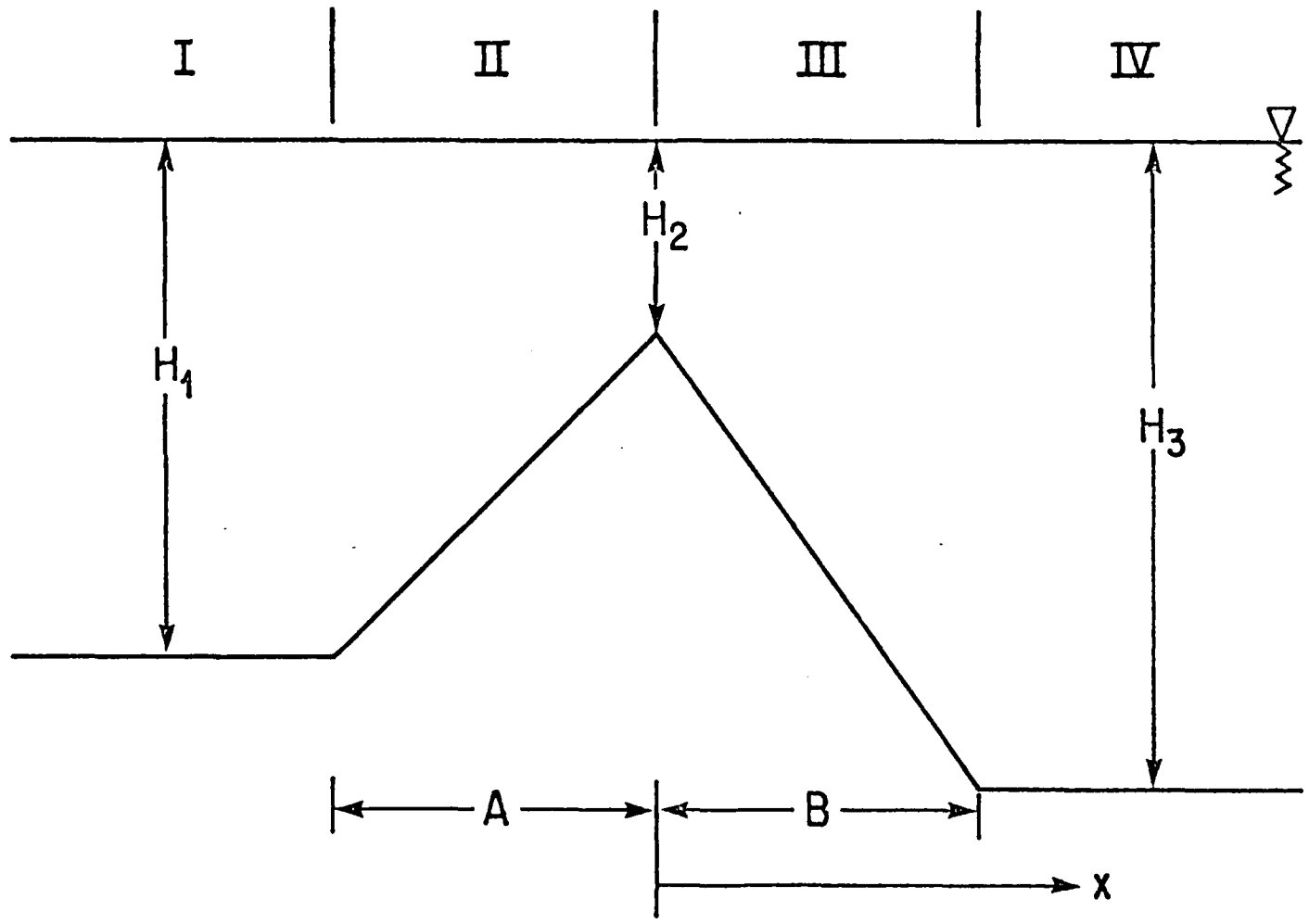

Figure 2

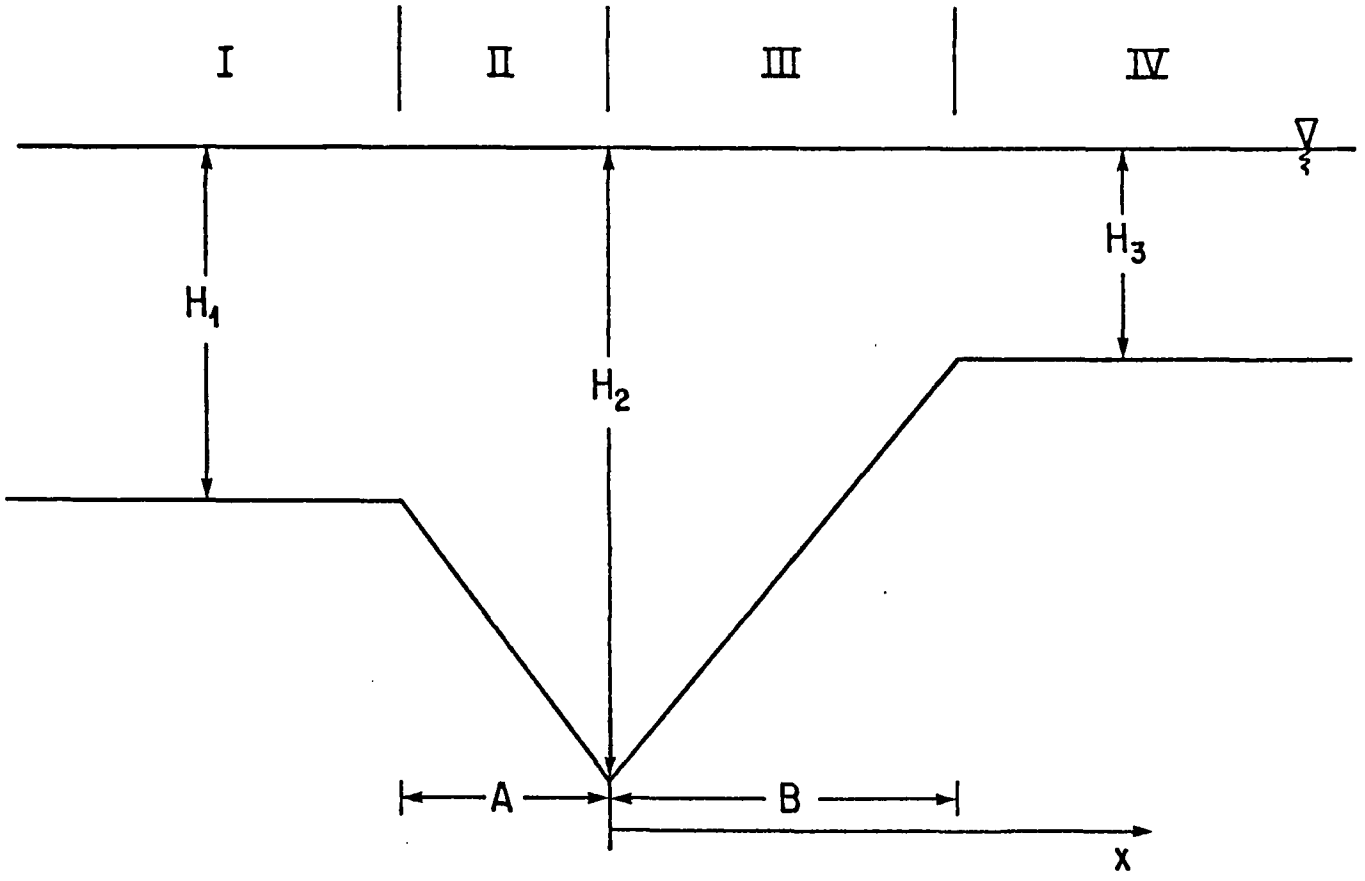

Figure 3

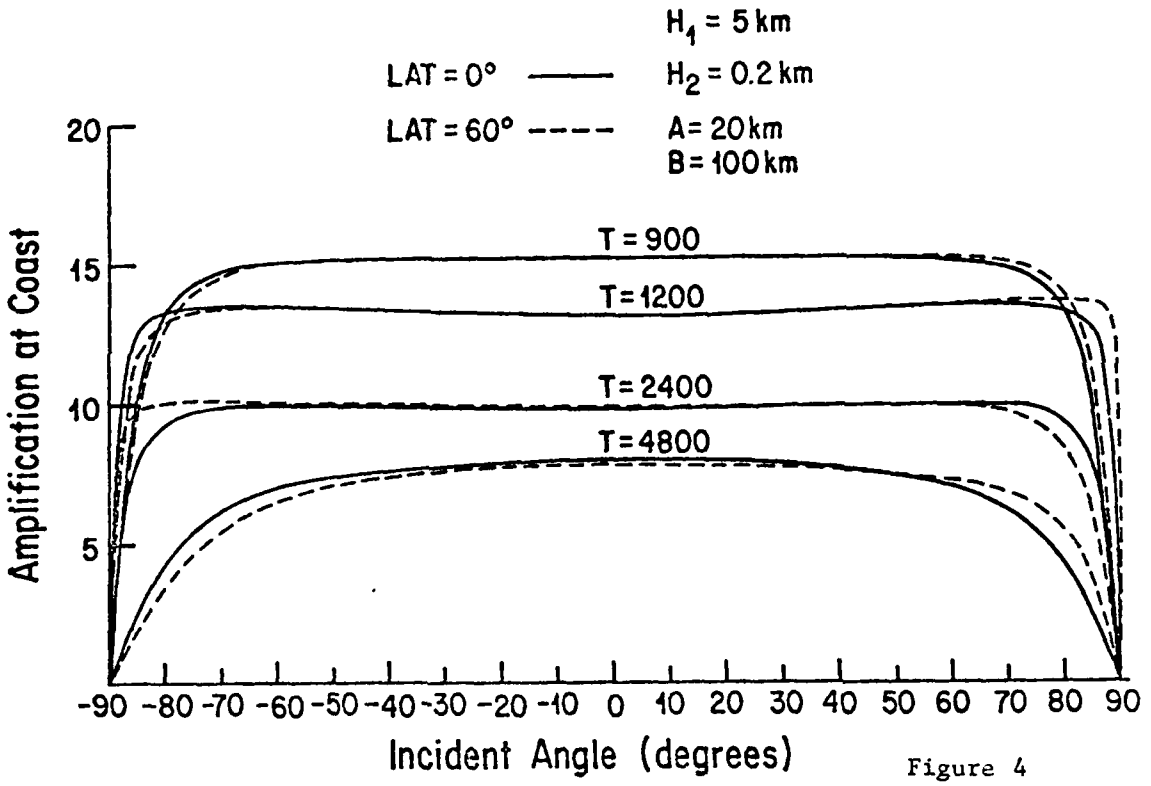

Figure 4

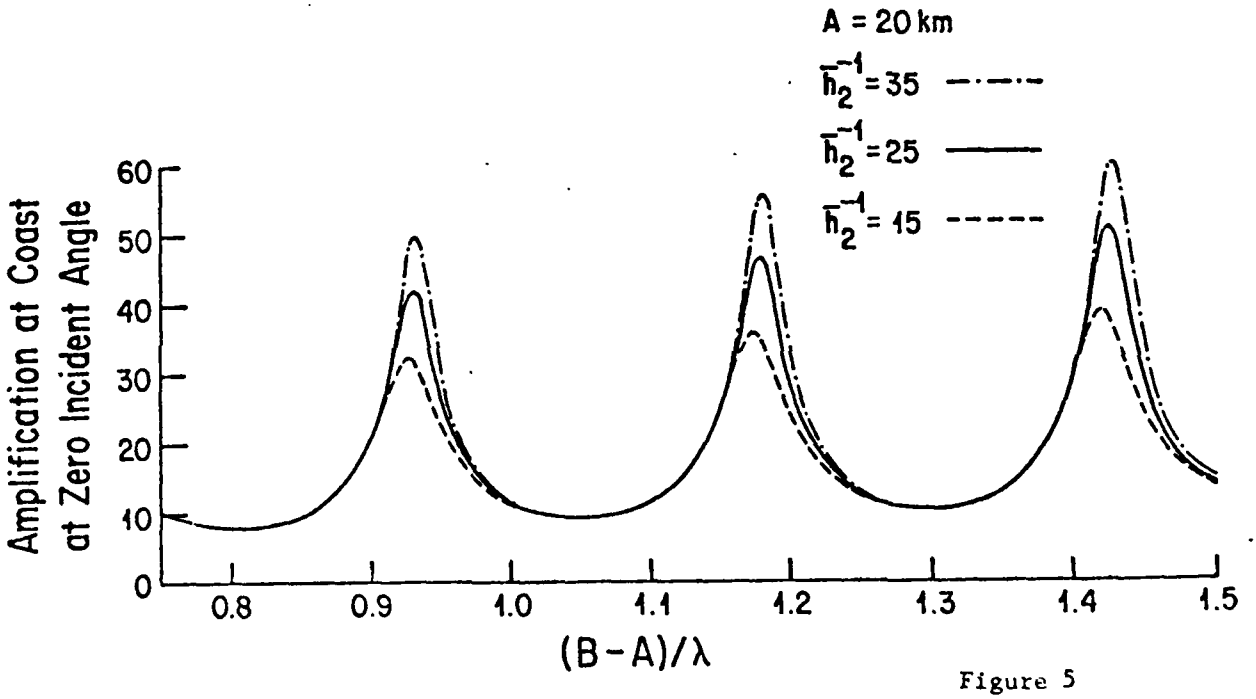

Figure 5

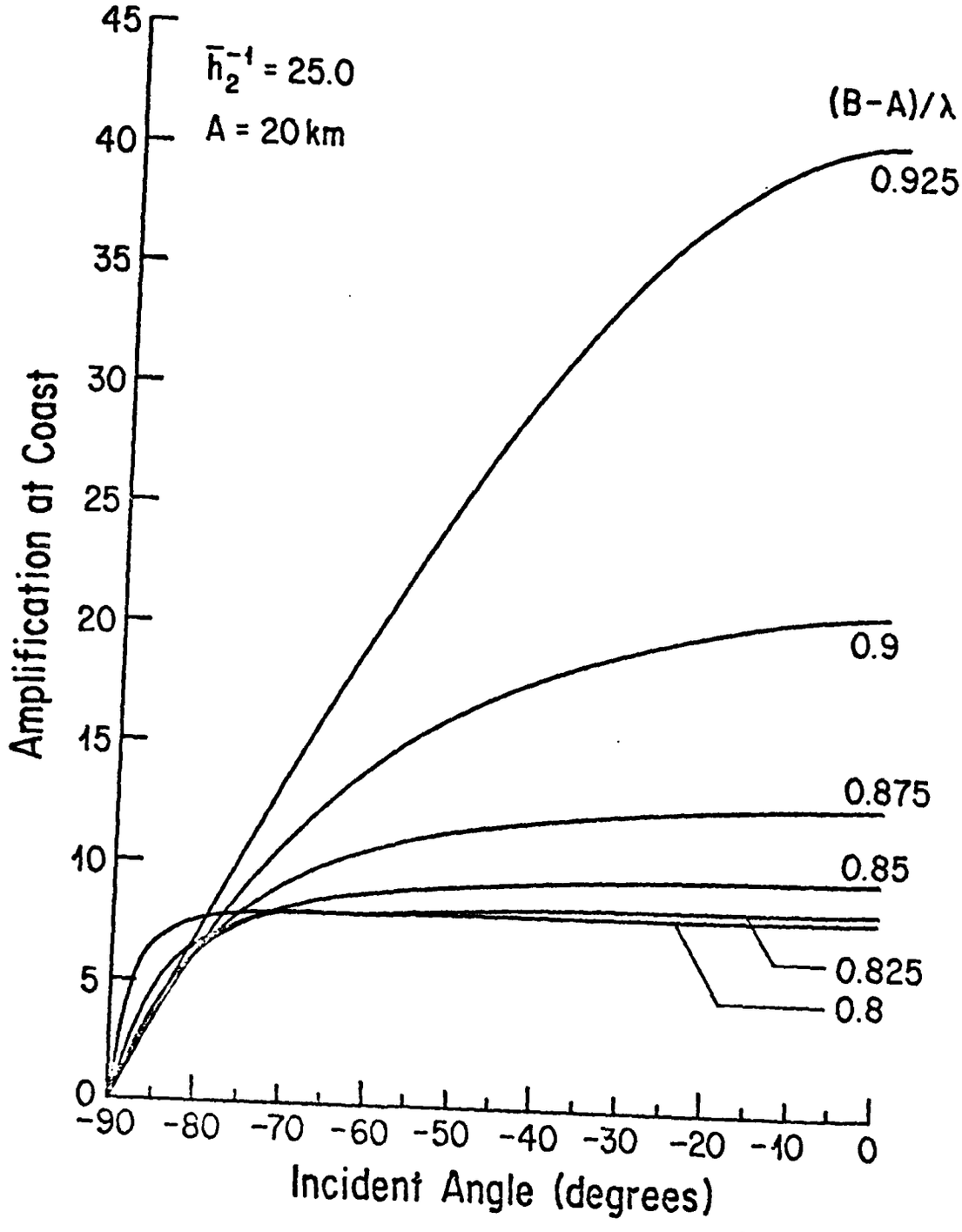
45
40
35
30
25
20
15
10
5
0
$\bar{h}_2^{-1}$ = 25.0
A = 20 km
(B-A)/λ
0.925
0.9
0.875
0.85
0.825
0.8
Amplification at Coast
-90 -80 -70 -60 -50 -40 -30 -20 -10 0
Incident Angle (degrees)

Figure 6

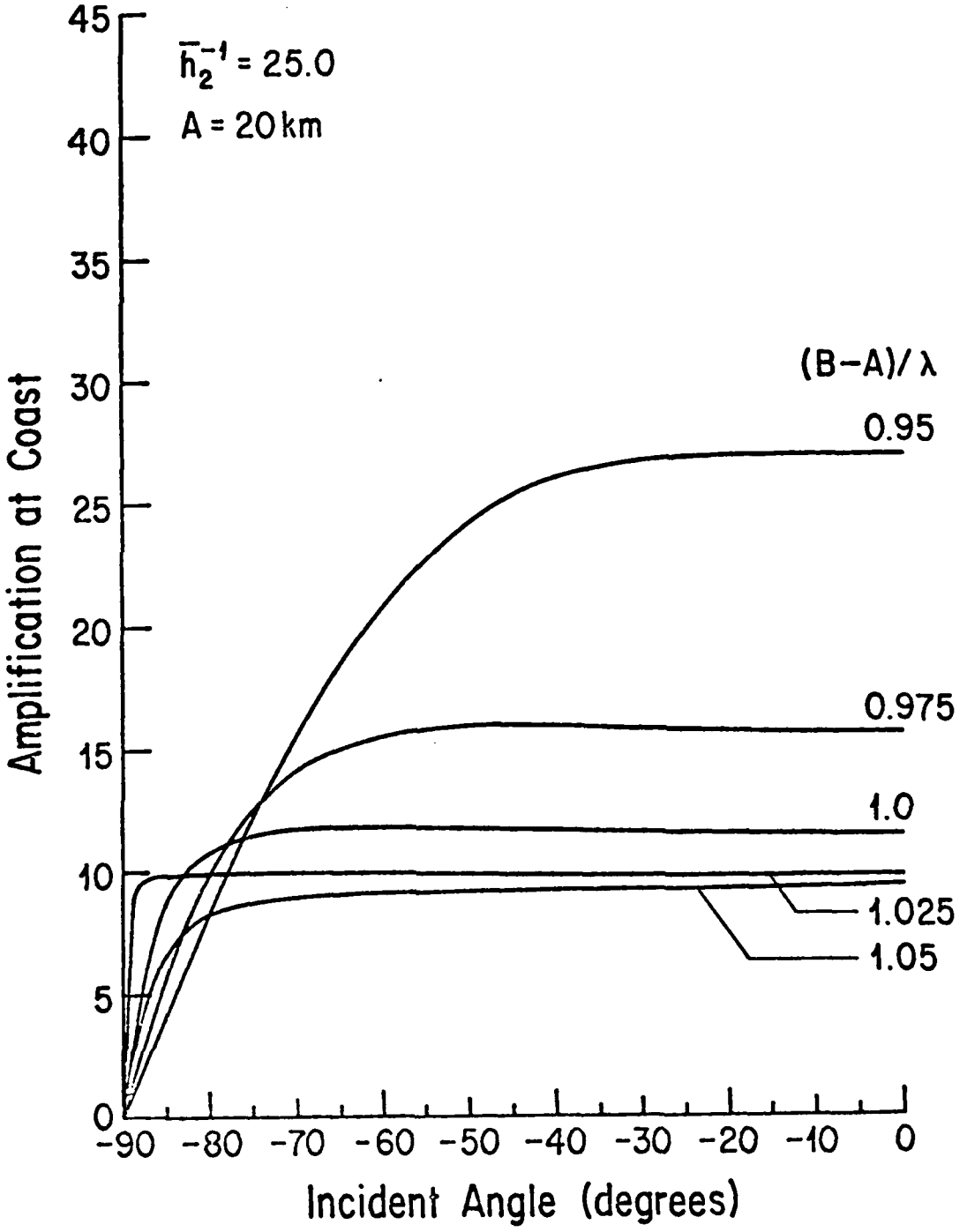
$\bar{h}_2^{-1} = 25.0$
A = 20km
(B−A)/λ
0.95
0.975
1.0
1.025
1.05
Amplification at Coast
Incident Angle (degrees)
45
40
35
30
25
20
15
10
5
0
-90 -80 -70 -60 -50 -40 -30 -20 -10 0

Figure 7

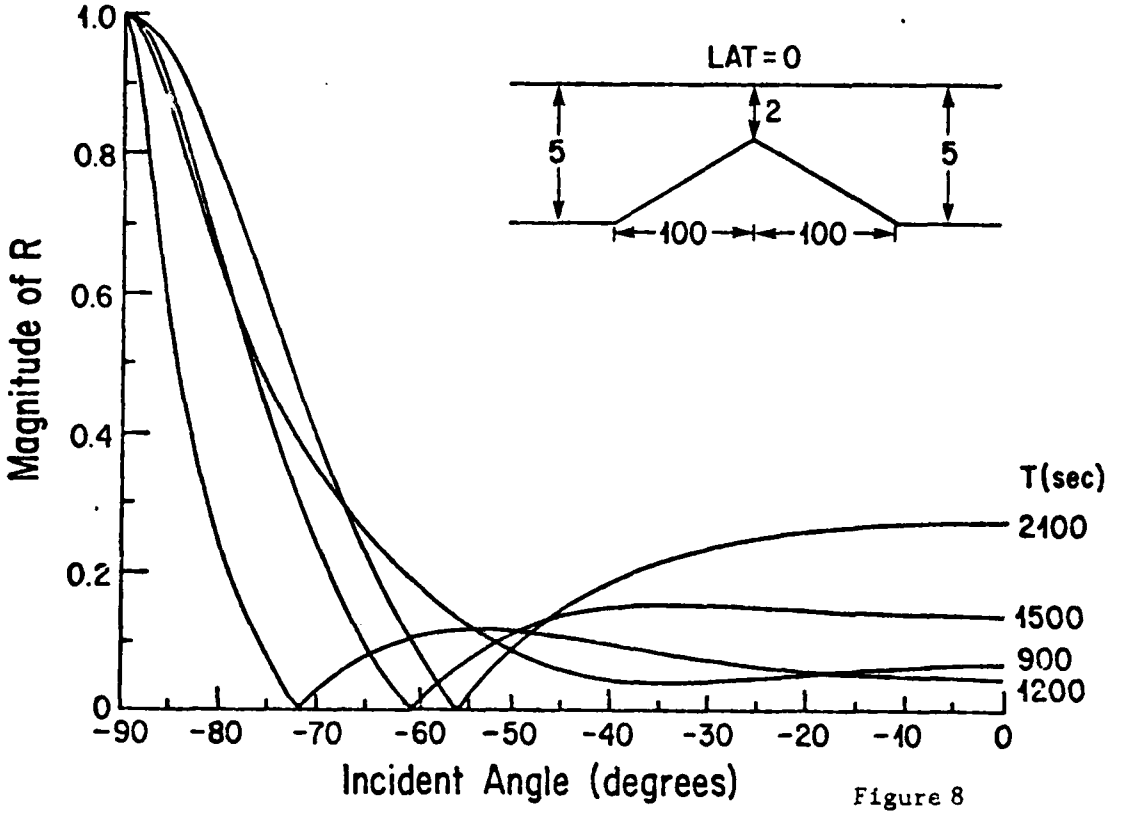

Figure 8

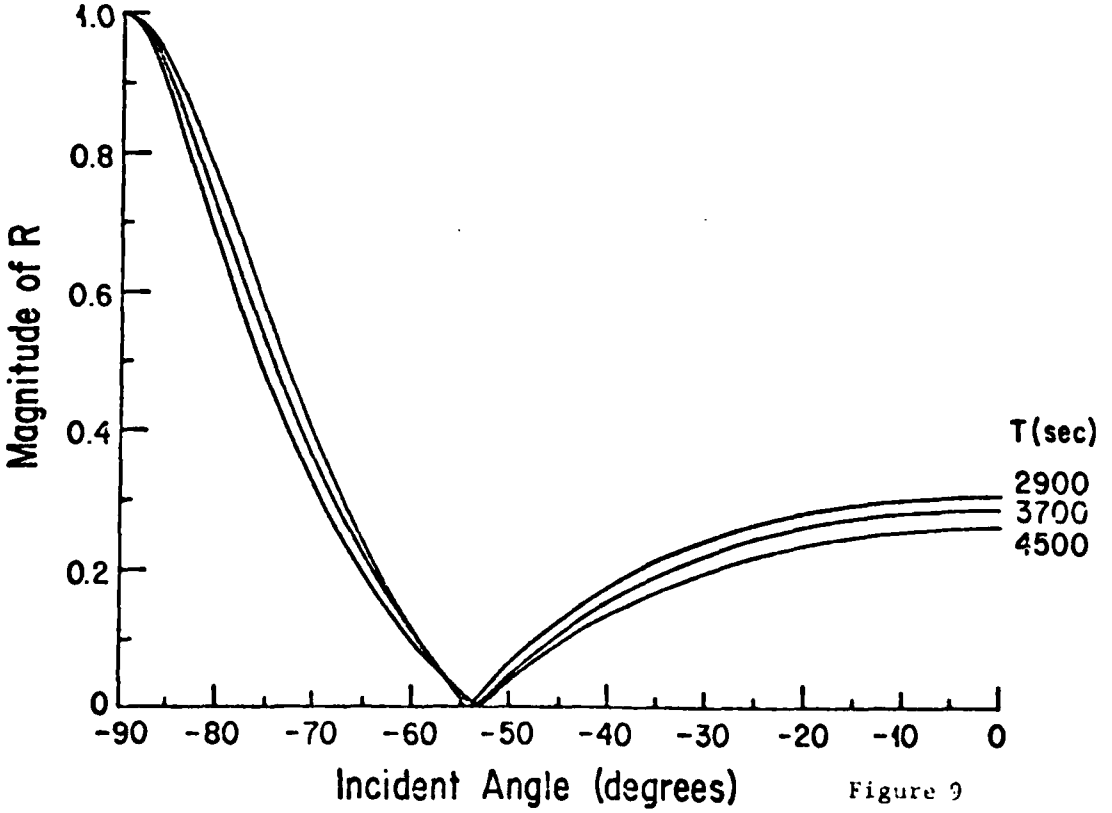

Figure 9

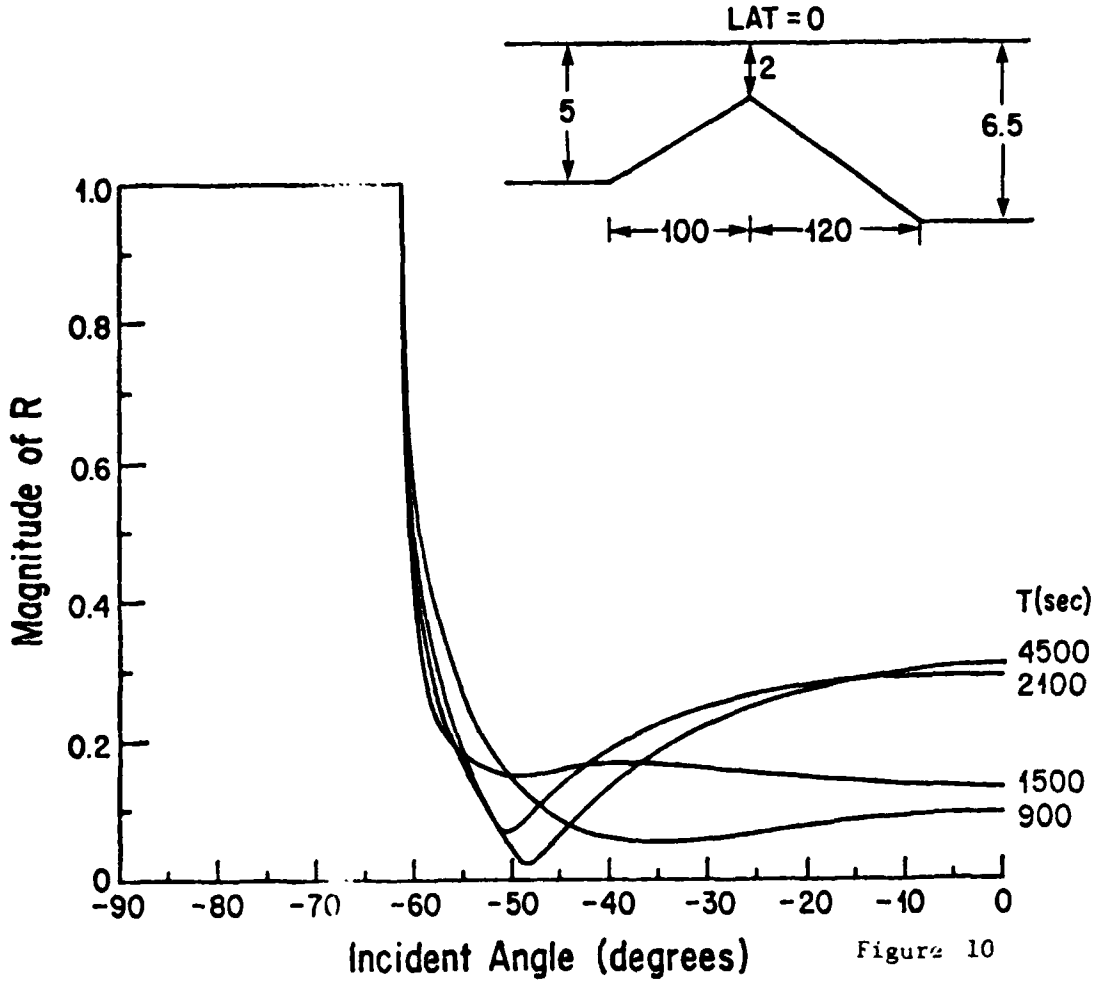
LAT = 0
5
2
6.5
100
120
1.0
0.8
0.6
0.4
0.2
0
Magnitude of R
T(sec)
4500
2100
1500
900
-90
-80
-70
-60
-50
-40
-30
-20
-10
0
Incident Angle (degrees)

Figure 10

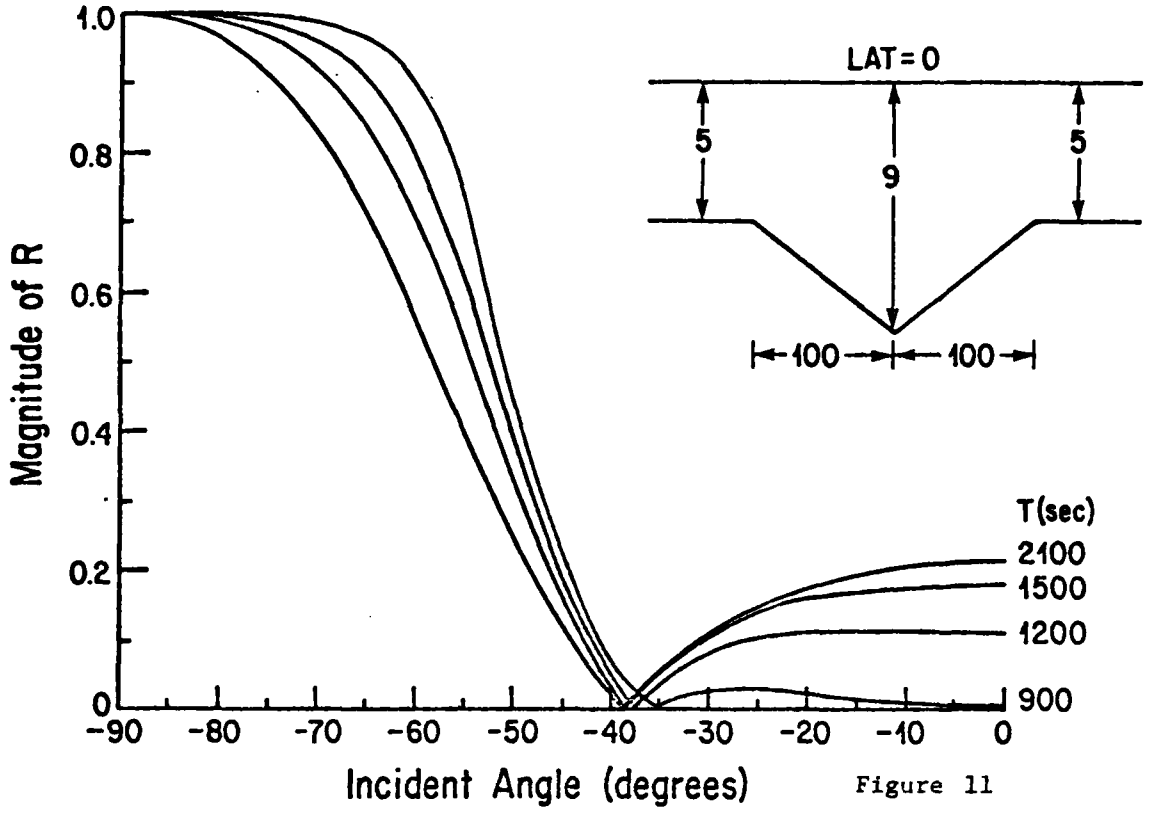

Figure 11

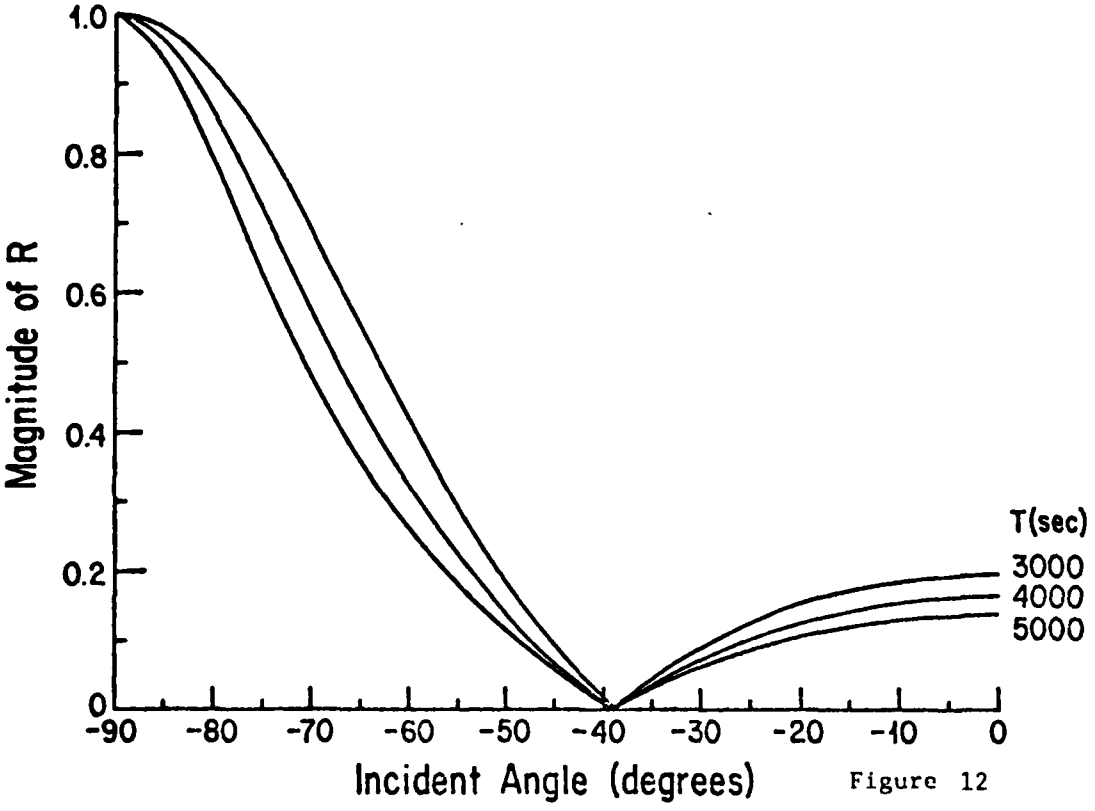

Figure 12

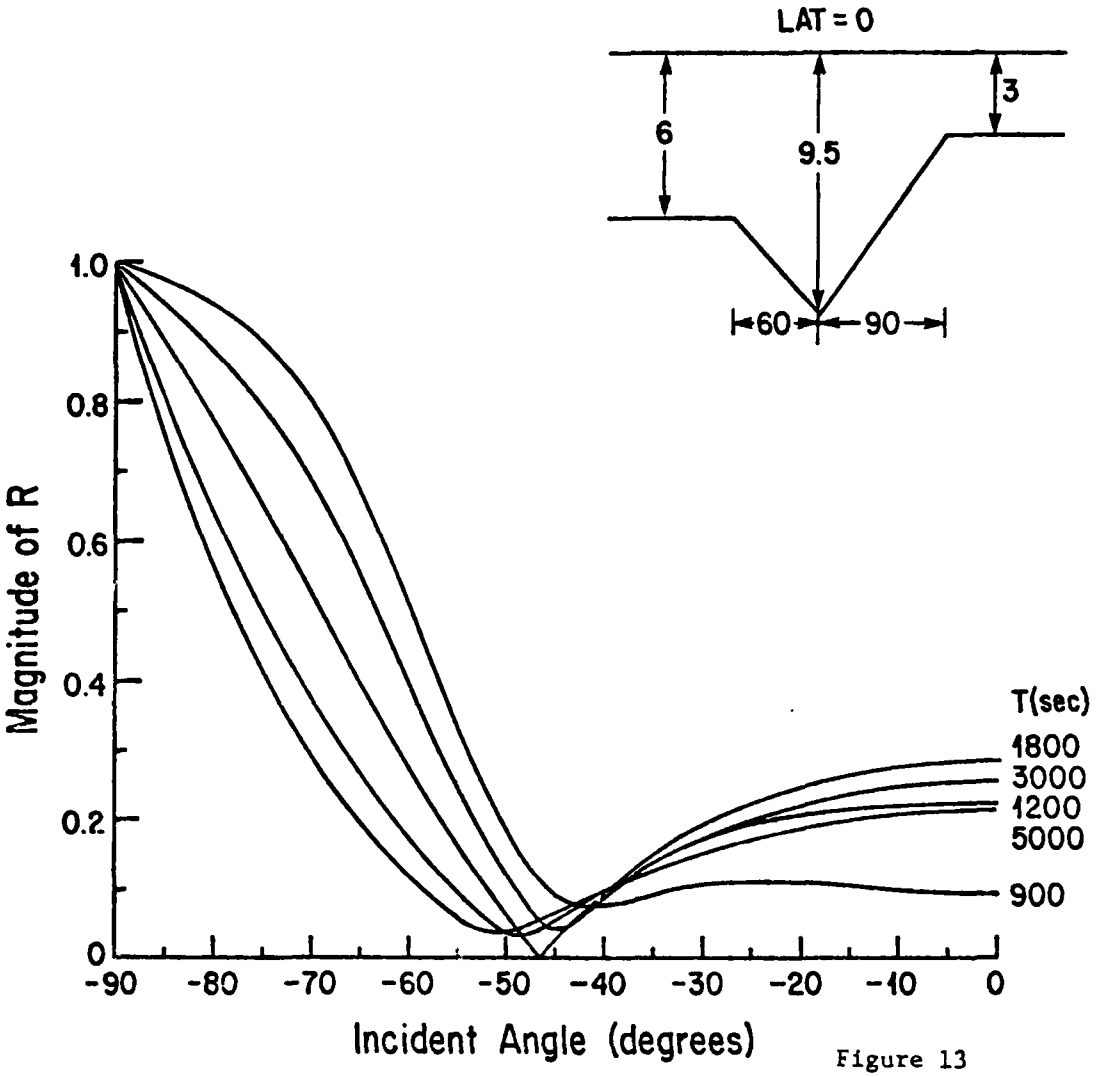
LAT = 0
6
9.5
3
60
90
1.0
0.8
0.6
0.4
0.2
0
Magnitude of R
-90
-80
-70
-60
-50
-40
-30
-20
-10
0
Incident Angle (degrees)
T(sec)
1800
3000
1200
5000
900

Figure 13

SECURITY CLASSIFICATION OF THIS PAGE (When Data Entered)

REPORT DOCUMENTATION PAGE

READ INSTRUCTIONS BEFORE COMPLETING FORM

1. REPORT NUMBER: 123	2. GOVT ACCESSION NO.: AD-A110880
3. RECIPIENT'S CATALOG NUMBER:	
4. TITLE (and Subtitle): Long Ocean Wave Scattering by Linear Segmented Topographies	5. TYPE OF REPORT & PERIOD COVERED: Technical Report
	6. PERFORMING ORG. REPORT NUMBER: 123
7. AUTHOR(s): W.L. Neu and R.P. Shaw	8. CONTRACT OR GRANT NUMBER(s): N0001479C0067
9. PERFORMING ORGANIZATION NAME AND ADDRESS: Research Foundation of the State University of New York at Buffalo	10. PROGRAM ELEMENT, PROJECT, TASK AREA & WORK UNIT NUMBERS: SUNY-B, 150-6292
11. CONTROLLING OFFICE NAME AND ADDRESS: ONR-PHYSICAL OCEANOGRAPHY Arlington, VA 22217	12. REPORT DATE: December 1981
	13. NUMBER OF PAGES: 20 Pages, plus 13 Figures
14. MONITORING AGENCY NAME & ADDRESS (if different from Controlling Office): N/A	15. SECURITY CLASS. (of this report): Unclassified
	15a. DECLASSIFICATION/DOWNGRADING SCHEDULE

16. DISTRIBUTION STATEMENT (of this Report)

Distribution is unlimited

17. DISTRIBUTION STATEMENT (of the abstract entered in Block 20, if different from Report)

" " "

18. SUPPLEMENTARY NOTES

N/A

19. KEY WORDS (Continue on reverse side if necessary and identify by block number)

Ocean Waves, Tsunamis

20. ABSTRACT (Continue on reverse side if necessary and identify by block number)

Problems of transmission and reflection of long, time harmonic, free surface gravity waves obliquely incident from a constant depth ocean upon linearly varying bottom topographies are considered. A solution to the vertically integrated dynamic equations over linear depth variation is developed in terms of Kummer functions. Coriolis effects are included but primary interest is on Class I (high frequency) long waves. Three cases are treated; the continental slope and shelf, the submerged ridge, and the submerged trench.

DD FORM 1 JAN 73 1473 EDITION OF 1 NOV 65 IS OBSOLETE

S/N 0102-LF-014-6601

Unclassified

SECURITY CLASSIFICATION OF THIS PAGE (When Data Entered)


DAT
FILM